Electronic Control of Site Selective Reactivity: A Model Combining Charge Migration and Dissociation

F. Remacle[†] and R. D. Levine*

The Fritz Haber Research Center for Molecular Dynamics, The Hebrew University Jerusalem 91904, Israel

E. W. Schlag and R. Weinkauf

Institut für Physikalische Chemie, TUM München, D-85747 Garching, Germany

Received: June 7, 1999; In Final Form: July 26, 1999

For large molecules, electronically excited states are denser than can be simply judged from the gap between the ground state and excited states. This is particularly true for large open shell systems, such as peptide cations. In such systems, short laser pulses can be used to prepare initial electronic states that are not stationary. These are non Born−Oppenheimer states, and therefore, the motion of the nuclei is not determined by a single potential. It is argued that such states could offer the possibility of control of reactivity. They can impede the usually facile vibrational energy redistribution, which is characteristic for a motion on a potential surface with a well. After a localized ionization, the dependence of site-selective fragmentation of small peptide ions on time is discussed with computational results based on a Pariser−Parr−Pople like electronic Hamiltonian. We predict a strong nonstatistical and site selective reactivity on a short time scale and also a dependence on the nature of the initial excitation. Results are presented for the fragmentation of Leu-Leu-Leu-Trp$^+$ and Ala-Ala-Ala-Tyr$^+$ ions and are compared with nanosecond laser pulse experiments.

1. Introduction

It is customary to begin discussions of molecular dynamics with the Born−Oppenheimer approximation. The motion of the nuclei can then be computed from a potential that is determined by the electrons. This potential is a function only of the positions of the nuclei. When the Born−Oppenheimer approximation fails, then as long as the failure is localized, one allows jumps from one electronic state to another, but between such jumps, the motion of the nuclei is still governed by a potential. In this paper we discuss why one may want an alternative point of view and what interesting features of the dynamics are brought to the fore if such a view is adopted. Specifically we will argue that there can be 'bypasses' in phase space which will take an energy rich polyatomic molecule from one region to another in a manner which is not quite so evident when one proceeds by the conventional approach.

The issue we discuss here is one of electronic control of reactivity. Energy rich large polyatomic molecules are notoriously poor at being directed.[1] Breaking a particular bond requires that enough energy is available at that site. But usually, any localized vibrational excitation rapidly dissipates over the numerous available vibrational states of the large molecule. This leads to the well-tested RRKM picture, where it is assumed that the excitation energy is first equilibrated and then dissociation takes place by a fluctuation[2] that localizes the needed energy in the bond that is to break. The larger the molecule, however, the rarer are the fluctuations that can concentrate enough energy in a single bond. Hence large molecules even far above their dissociation threshold are expected to have a kinetic stability: To detect fragment ions, dissociation of the energy rich parent ion needs usually to occur on a μs time scale or faster. This narrow detection window is the origin of the kinetic shift,[3] i.e., the appearance of fragments only at energies higher than the threshold dissociation energy. This means that very large ions even at high internal energies should not dissociate in the time window of a mass spectrometer.[4] This, however, is contrary to experiments, where facile fragmentation is observed already at 4.5 eV internal energy.[5−7] Hence there must be a route that circumvents fast energy dissipation. In open shell systems, we suggest that this can be an electronic effect, as qualitatively discussed in section 2 and is clearly seen in the computations reported below.

There is currently a rich literature seeking ways to overcome the fast intramolecular vibrational energy redistribution (IVR), see ref 8 and references therein. That there has to be some way around facile IVR follows from experiments that show that for some molecules the rate of dissociation does not decrease exponentially with increasing size of the molecule.[4,9] It indeed appears that on one hand there are bottlenecks, which slow the vibrational energy flow and on the other hand that there can be extreme motion states,[10,11] whose excitation leads to ultrafast dissociation. So it is not categorically the case that energy equilibration must precede dissociation when the nuclear motion occurs on the ground potential energy surface.

We have recently explored[7,12] a different approach to steering the reactivity of large ions, which involves electronic effects. It avoids the issue of fast IVR by not making the energy available to the nuclei until it is needed for dissociation. The assumptions of this model are (i) the electronic state density is high, as calculated here by the PPP theory; (ii) the electronic states that are used to describe the time evolution are diabatic states with a nonuniform charge distribution; (iii) the (diabatic) interstate coupling is included and this allows charge to migrate,

* Corresponding author. Fax: 972−2−6513742. E-mail: rafi@fh.huji.ac.il.
[†] Chercheur Qualifié, FNRS, Belgium. Permanent address: Département de Chimie, B6b, Université de Liège, B4000 Liège, Belgium.

10.1021/jp991853k CCC: $18.00
Published on Web 09/03/1999

(iv) the initial state depends on the pulse duration of the excitation, and (v) prompt dissociation takes place from those diabatic states which are directly coupled to the possible dissociation channels.

We here discuss the essence of this approach and emphasize the key ingredients. To make the discussion concrete we compare the calculations to the observed fragmentation pattern in ns laser excitation experiments on two peptide cations, which exhibit a very different dissociation pattern. It has been shown previously[5−7] that in peptide cations the fragmentation patterns can be understood as a charge induced process governed by local ionization and local dissociation energies.[5] The initially localized (positive) charge migrates. At the site where the charge is, the bond is weaker and dissociation is then possible. Hence the picture is a nonstationary one where "reactivity follows charge". The model presented here explicitly takes into account the charge migration through the dense manifold of electronic states. As such it is quite different than a conventional RRKM picture. We do, however, retain a local version in that the rate of dissociation from a given electronic state is governed by the locally available energy.

The purely electronic state description that we use is oversimplified in that we do not explicitly discuss such important aspects as the role of Franck−Condon overlap on charge hopping. Rather, we use the magnitude of the charge-transfer amplitude as a parameter, which sets our time scale. The advantage of the model is that it discusses in one framework charge mobility and reactivity. The following points can be derived from this model: (i) prediction of an "electronic trapping" effect, which circumvents energy dissipation; (ii) prediction and simulation of site-selective electronic controlled dissociation in the short-time regime after excitation; and (iii) converges for larger times to the time-averaged fragmentation pattern as observed in nanosecond laser excitation mass spectrometry. Although these conclusions are based on a model, they show that new ways can exist for large complex systems to circumvent dissipation of the energy into vibration.

Specifically, we compare the computation of the model with the observed fragmentation pattern for ns laser ionization of Leu-Leu-Leu-Trp and Ala-Ala-Ala-Tyr. Both peptides have a chromophoric amino acid at the C end (tryptophan, Trp, or tyrosine, (Tyr) and nonaromatic amino acids (leucine, Leu, or alanine, Ala) at the N terminal and along the chain. The experimental results exhibit two features: (i) Even though ionization occurs at the C terminal (the chromophore end), fragments can be formed which stem from the (positive) charge being on the other side of the peptide (N terminal mass 86 Dalton for leucine and mass 44 Dalton for alanine). (ii) The fragmentation pattern can differ depending on the composition of the peptide.

Result i shows that charge migration is present in such systems since the N terminal dissociation must occur from a precursor state which has a predominant positive charge distribution at the N terminal. Result ii can be understood on a basis of a local picture where the energetics are determined by the local charge state. That is, the dissociation energy of the bond is lowered when the charge is adjacent and this energy can be different for, say, Leu^+-Leu-Leu-Trp and Leu-Leu-Leu-Trp^+. Neglecting any coupling between the adjacent amino acids and using a local ionization potential (IP) of Leu, Ala, Tyr, and Trp as[6] 8.5 eV, 8.6, 8.0, and 7.5 eV, one can obtain a zeroth-order estimate of the energies of different ions. Using local dissociation energies in the presence of the charge of 0.5 eV at the N terminal and 1.5 eV at the C terminal, as suggested by Weinkauf et al.,[5] one obtains for the Leu-Leu-Leu-Trp cation N and C terminal dissociation thresholds of 9.0 eV with respect to the neutral ground state. Hence, dissociation is expected to occur at both ends. For the other parent cation, Ala-Ala-Ala-Tyr, the N and C terminal dissociation thresholds are 9.1 and 9.5 eV, respectively. Hence, in this zeroth-order picture, fragmentation of the Ala-Ala-Ala-Tyr ion should be favored at the N terminal. The object of the model computations is to provide a detailed picture. First, we determine the energetics including the (diabatic) electronic site−site coupling that is necessarily present so as to induce charge migration. The values of the local IPs that we use, Table 1, are those of ref 6. This means that we use a somewhat higher IP for an amino acid when it is at the N terminal than that when the amino acid is in the middle of the chain, see Figure 4 and Table 1. Also, we here compute the bond breaking energies by separately computing the energies of the fragments. The dynamical computations follow the time evolution of the energy rich molecule so as to explore the competition between charge migration and dissociation, since dissociation occurs from where the charge is. Finally, the detailed model explicitly introduces the coupling to the dissociation channels.

TABLE 1. Parameters of the Hamiltonian (3.4)[a]

energy site	α (local IP)	I	γ
Leu	−36.0 inside, −34.0 end	1.0	Leu-Leu: 1.0
Trp	−30.0	0.4	Trp-Leu: 1.0
Ala	−36.8 inside, −34.4 end	4.0	Ala-Ala: 1.0
Tyr	−32.0	0.8	Tyr-Ala: 1.0

[a] All energies are in units of β. Time is therefore scaled by $1/\beta$. The values of the local ionization potentials, (the α's), shown in Figure 4, which are those proposed by Weinkauf et al., ref 6, correspond to $\beta =$ 0.25 eV.

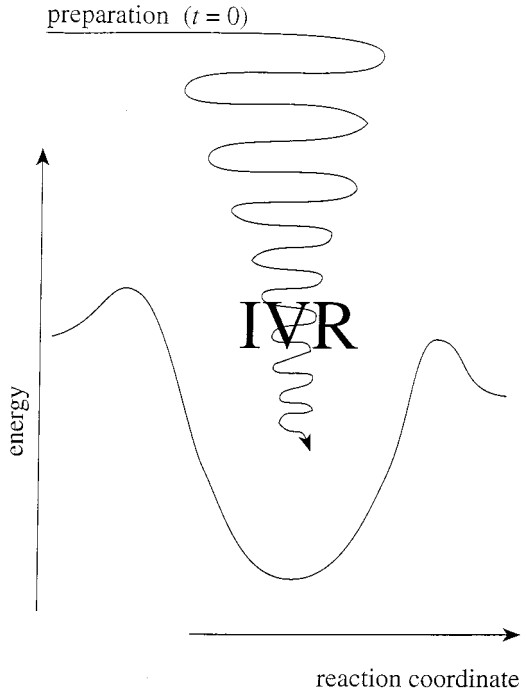

Figure 1. The potential cut along the reaction coordinate for a system with a well, here the chromophore cation ground state. The RRKM picture assumes that the system is delayed in its motion along such a potential because of intramolecular vibrational energy transfer to other degrees of freedom (IVR) which are not shown in such a plot. Whereas the total energy is conserved, the IVR reduces the energy along the reaction coordinate to such an extent that the motion is confined to within the well.

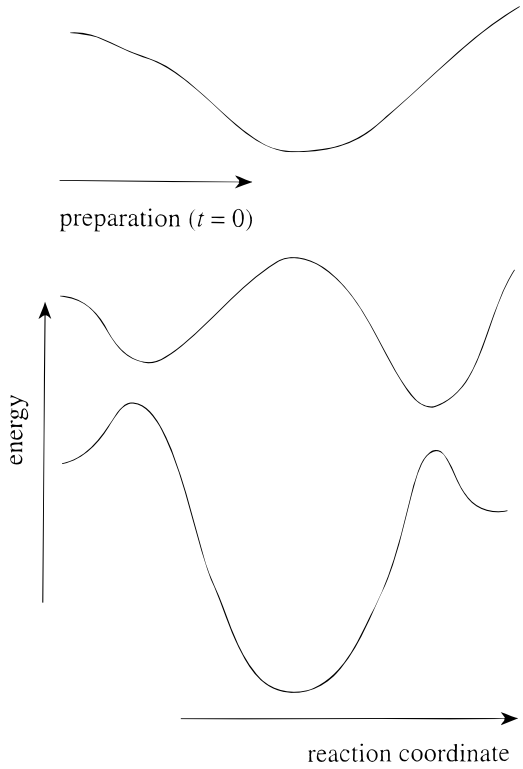

Figure 2. The potentials along the reaction coordinate for a three electronic state problem. The plot is drawn using the rule of thumb that barriers along the ground-state potential are correlated (cf. Figure 4) with dips in the excited-state potentials and vice versa. The figure is still incomplete in a very essential way; it shows the variation along the reaction coordinate but it does not show the dependence on the other nuclear modes.

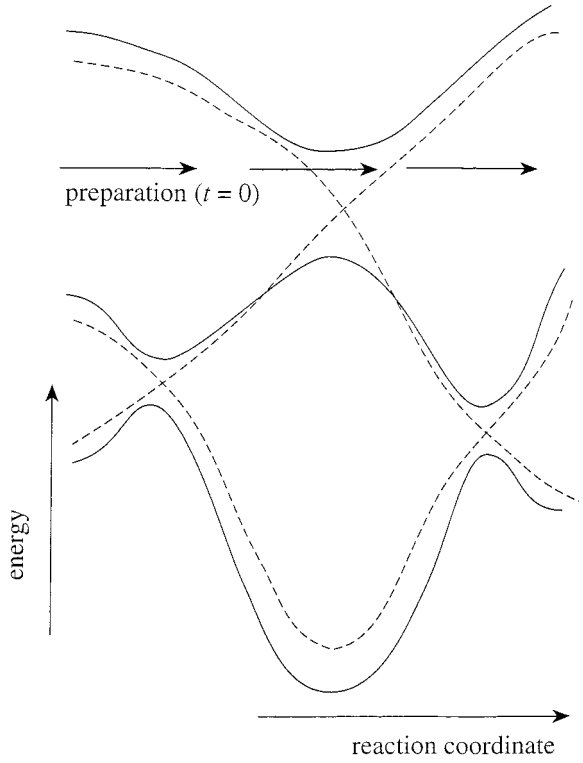

Figure 3. The diabatic potentials (dashed lines) along the reaction coordinate for a three electronic state problem. The adiabatic potentials, same as in Figure 3, are shown as solid lines.

Section 2 is a general qualitative discussion of why diabatic electronic states offer a way around energy dissipation into the many nuclear modes, thereby allowing for prompt dissociation. Section 3 specifies the key details of the electronic Hamiltonian. The electronic structure of the products is discussed in section 4 and the bound-continuum coupling in section 5. Computational results and their interpretation are given in section 6. The nanosecond laser pulse experiments on peptide cations, experiments that gave rise to observations i and ii above, are discussed in section 7.

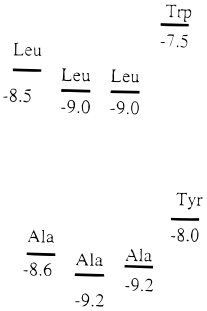

Figure 4. The relative site IPs[5,6] (in eV. In the computations and in Table 1 we report all energies, and time, in units of β. The results shown in this figure correspond to $\beta = 0.25$ eV.) for the two peptide chains used in the computations. The IP of the N terminal differs slightly to the IP in the peptide bonds. Note that the chromophore beside the ground state has also excited states. Further on in a molecular orbital picture in the peptide bond two degenerate states are present. For simplification we confine our calculations on four sites (three nonaromatic sites and the chromophore ground-state site).

2. Qualitative Considerations of the Role of Several Electronic States

Figure 1 is a traditional picture of the potential energy along the reaction coordinate when there is a deep well in the middle. This is the kind of energy profile that favors the formation of a long living intermediate: Coming from the left, one has enough energy to cross the first barrier and hence one could proceed directly to cross the other barrier and promptly exit as products. The reason for any delayed exit is that the figure fails to note the presence of the many other degrees of freedom that are coupled to the reaction coordinate. In the region of the deep well, enough energy can flow into these other modes so that the energy of the motion along the reaction coordinate is not sufficient for an exit. The motion is, temporarily, bound in the well. The delay is finite because energy will eventually flow back to the reaction coordinate so that dissociation can take place. The exit will be to the left or to the right depending on the barrier heights and on the tightness of the respective transition states, but it will be largely independent of which side the entrance to the well was made.[13,14]

Figure 1 is drawn for a bimolecular collision. In a unimolecular reaction one begins with the system which is already in the well region. Given enough energy it can exit in either direction but it will be delayed in doing so unless the energy of excitation is directly made available to the motion along the reaction coordinate.

For either the unimolecular or the bimolecular access to the well region, there appears to be no simple way of constraining the energy to remain in the reaction coordinate. Of course, in the bimolecular mode, if the initial collision energy is quite high, when the system crosses the well, draining some energy into the other modes will still not trap the motion in the well. One therefore expects that at higher energies the collision will become direct.[15] If one could very suddenly pump lots of energy into a molecule then a prompt unimolecular dissociation is also

conceivable. The rough estimate rate $\propto((E - E_0)/E)^{s-1}$ shows that for a large molecule (of *s* modes), the energy *E* needs to be very much higher than the barrier energy E_0 for a prompt process.

Figure 2 is a more elaborate way of plotting Figure 1. It shows not only the potential of the ground electronic state but also the potential along the reaction coordinate of two excited states. It is clear that at a higher energy one can no longer restrict attention to a motion confined to the ground electronic state. On the other hand, one need not assume that hops to the excited state will occur as soon as they are energetically allowed. The motion of the nuclei is subject to the Franck−Condon limitations, which exponentially disfavor large changes in the momenta of the nuclei.[15]

Figure 3 is an alternative way of plotting Figure 2. Shown as a dashed line is the electronic energy of the diabatic electronic states. It offers a key to a possible route for selectivity. By one transition between two different electronically diabatic states it is possible to transverse the region of the deep well without having energy made available to the nuclear motion. Energy is, of course, conserved, but Figure 2 suggests that in the well region energy could be stored as electronic excitation rather than as energy of the nuclear motion. This requires of course, that the diabatic description is a valid zeroth-order picture because, otherwise, electronic−nuclear coupling will dissipate the electronic energy which is the conventional assumption in the quasiequilibrium theory of mass spectra.[16]

The diabatic and the adiabatic (=Born−Oppenheimer) pictures are complementary. A nonadiabatic transition means that the system remains on the same diabatic state while a transition between two diabatic states is a motion on the same adiabatic state. The suggestion made in Figure 3 can equally well be made by stating that two non adiabatic transitions, one in the vicinity of each barrier, allow the system to cross the well region with little energy being available for dissipation. In the diabatic picture shown in Figure 3, the well region is crossed by one or more transitions between diabatic states.

Strictly speaking, the sequence of events is two nonadiabatic transitions, one in the vicinity of each barrier, and an adiabatic behavior in the well region. We would all agree with an adiabatic behavior in the well region but this is equivalent to a transition between two diabatic states, as shown in Figure 3. What one is less likely to have agreement on are the two nonadiabatic transitions in the region of the two barriers. Such transitions are not likely to be effective unless the gap between the two Born−Oppenheimer states is not large. Hence, for the proposed mechanism to be truly effective, one must initiate the dynamics in an electronically diabatic state.

The diabatic state picture suggests not only that one can coherently cross the well region but also that energy is available for barrier crossing. This is because the diabatic state is repulsive in the exit region and so the motion toward products should be quite prompt.

The proposed mechanism relies on more than one stationary electronic state taking part in the dynamics. A linear combination of electronic states is a nonstationary state. Such a state does not have a sharp value for the electronic energy and, as time evolves, the different components acquire a different phase. So after a while the motion on the different states will decohere and eventually one will reach the, so-called, quasi-equilibrium, limit of mass spectrometry[16−18] or its RRKM equivalent for neutral molecules.[19] In this paper we examine the earliest time period and drastically simplify the picture by centering attention only on the electronic aspects of the problem. Dissociation is accounted for in a manner suggested in Figure 3: Certain diabatic states are allowed to exit to the continuum, which we mimic by endowing them with a decay width. The precise specification of the width is not trivial because the products themselves can have more than one electronic state. This is discussed in section 5.

3. Electronic Problem

We use the simplest possible description where each amino acid is a 'site' having one orbital. A tetrapeptide is then a chain of four sites. The site energies, which are the ionization energies of the amino acids, need not be the same, cf. Figure 4 below. The diabatic states are the suitably antisymmetrized states made up from these uncoupled site orbitals. The diabatic states are coupled in a manner that allows charge to move between adjacent sites. Diagonalizing this coupling leads to molecular states that are the Born−Oppenheimer states, i.e., eigenstates of the electronic Hamiltonian. If the site energies are all equal then the molecular states will invariably be delocalized, thereby allowing the charge to coherently migrate along the chain.

Two factors act against the migration of charge. One is that the site energies are not all equal. This effect can be described in a single electron approximation.[12] It explains why substitution of one amino acid by another can hinder charge migration. In the present study we also penalize an electron that moves to a site which is already occupied (by an electron of a different spin). In solid state physics this is known as a Coulomb blockade and is usually described by a so-called Hubbard Hamiltonian.[20,21] In molecular physics this is known as a Pariser−Parr−Pople type Hamiltonian.[22−24] The latter is actually a better approximation, because it also allows the polarization of one site by an electron on an adjacent site. Sometimes, the self-and cross terms are referred to as the capacitance terms. Even this modest model gives, in a four-site problem, 20 different doublet electronic states of the radical ion, eight of which (listed in eq 3.1 below) correspond to a removal of an electron from the right end (which we take to be the chromophore end).

Without the Coulomb blocking there is no energy penalty to having more than one electron per site. The result is that such states (called "ionic") are degenerate with other states where the charge is more uniformly distributed. Because of this degeneracy, ionic and covalent states can have the same weight. This is a long known[25] fault of molecular orbital theory, a fault that is not fatal unless one needs to allow for dissociation, which we do. Without the Coulomb blocking one cannot correctly describe the dissociation channels. In a molecular orbital description, H_2 for example, will dissociate with equal probability to H + H and to $H^+ + H^-$. Including the Coulomb repulsion is necessary for a qualitatively correct description of the possible fragments. In the H_2 example, the repulsion makes the threshold for dissociation into the ionic states higher by the energy *I*. For this reason, the Coulomb repulsion energy, which is a property of a site, can be estimated[26] as the energy threshold for charge disproportionation, site + site → $\text{site}^+ + \text{site}^-$. For our model it means that different amino acids can differ quite a bit by their value of *I*. Another way of understanding *I* is to think of it as the "charging energy" of a site, namely, the capacity of a site to accommodate an extra electron.

Technically, the set of diabatic states that we use is a set of orthogonal electronic states that are spin adapted antisymmetrized products of the single electron site orbitals. We call it the site basis. In a very technical language, this basis diagonalizes the weight generators,[23,27] which specify the electronic charge on any one of the different sites. The further advantage

is that this basis also diagonalizes the repulsion between two electrons on the same site. This basis does not diagonalize the coupling of the sites by the charge transfer so that the basis states are not the familiar stationary electronic states.[7,28,29]

The site electronic basis is the technical expression of the "local" description of the experiments of Weinkauf and Schlag. As an example, we write down symbolically the eight different site basis doublet states that are possible for a radical cation of four sites with there not being an electron on the rightmost site

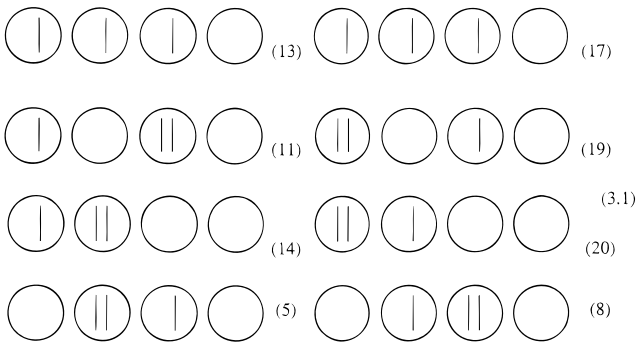

(3.1)

Note that we represent the electrons by a rod and not by an arrow. This is because we do not specify the spins of individual electrons but only the total spin of the state (a doublet) and the occupancy (as shown in (3.1)). The explicit construction of this basis is given elsewhere.[27] The numbering of the states shown in (3.1) is arbitrary.

The (zeroth-order) energies of the eight states shown in (3.1) are easy to compute even when Coulomb blocking is included

$$E = \sum_{i=2}^{4} n_i(IP)_i + (1/2)\sum_{i=2}^{4} (n_i^2 - n_i)I_i \qquad (3.2)$$

Here i is an index of the orbitals, IP is the local ionization potential, and I is the repulsion between two electrons when they are on the same site. Note that the zero of energy for the electronic Hamiltonian is different from the threshold energies used in the experiment, which is the ground state of the neutral. In (3.2) and (3.4), the zero of energy is the four ionized and noninteracting sites. This means that the electronic energies will be negative.

Not included in (3.2) is another effect namely the cross polarization. Thinking of I as a capacitance term, the missing contribution in (3.2) is that of an electron on a given site polarizing the adjacent sites. In electrostatic terminology, this is a repulsion between electrons on adjacent sites. This coupling, which is allowed for in the Pariser−Parr−Pople type Hamiltonian, (3.4) below, is diagonal in the site basis and so including it requires no additional computational effort. In conclusion, the site basis, which we regard as the set of diabatic states of the problem, diagonalizes the electrostatic effects. The only nondiagonal term of the electronic Hamiltonian is the transfer of charge between adjacent sites.

The eight states shown in (3.1) form two bands. Two degenerate states of lower energy (states 13 and 17 above) in which each electron is on a different site so that there is no repulsion contribution in (3.2) and six ionic states at a higher energy. The six ionic states are not all degenerate because the terminal amino acid at the N end has a slightly higher IP, cf. Figure 4. The energy gap, due to the repulsion, between the covalent and ionic states, will turn out to be an important consideration in what follows.

The adiabatic states are obtained by diagonalizing the electronic Hamiltonian, including the charge-transfer coupling. For the four-site cation there are twenty possible site states. Eight are shown in (3.1). These are the eight states with no charge at the C end. By symmetry, there are eight states with no charge at the N end. These are the mirror image of the states shown in (3.1). The careful reader will note that of these eight, two (which are those shown in the bottom row in (3.1)) are common to both sets. So there are 14 states that can correlate with states of ionic products for dissociation at either the C or the N end. More on this in section 4 below. Six site states have charges at both ends. They are shown in (3.3)

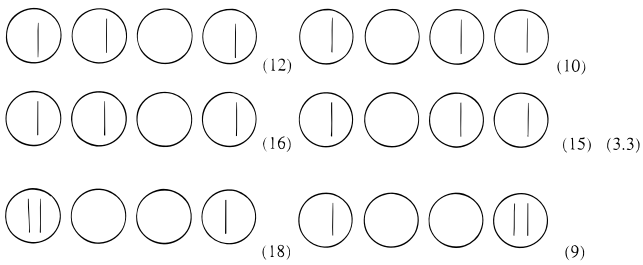

(3.3)

Of these six site states, four, shown in the top two rows, are covalent. The rest are ionic in that one site has two electrons.

The electronic Hamiltonian is given by

$$H = \sum_{i=1}^{4} \alpha_i \hat{E}_{i,i} + \beta \sum_{\substack{i\neq j=1 \\ i=j\pm 1}}^{4} \hat{E}_{i,j} + \frac{1}{2}\sum_{i=1}^{4} \hat{E}_{i,i}(\hat{E}_{i,i} - 1)\, I_i + \frac{\gamma}{2} \sum_{\substack{i\neq j=1 \\ i=j\pm 1}}^{4} \hat{E}_{i,i}\, \hat{E}_{j,j} \qquad (3.4)$$

where $\hat{E}_{i,i}$ is the operator that determines the charge on site i and β is the amplitude for charge transfer between adjacent sites. The operator that moves the charge is $\hat{E}_{i,j}$. Unlike $\hat{E}_{i,i}$, $\hat{E}_{i,j}$ is not diagonal in the site basis. It represents the coupling of the diabatic states. Explicitly, the operators $\hat{E}_{i,j}$ are defined in terms of the creation (annihilation) operators $a^{\dagger}_{i,\mu}$ ($a_{i,\mu}$) of the orthonormal site spin−orbitals $|i\mu\rangle = |i\rangle|\mu\rangle$, $i = 1, ..., n$ and $\mu = \pm 1/2$

$$\hat{E}_{i,j} = \sum_{\mu}^{2} a^{\dagger}_{i,\mu} a_{j,\mu}, \quad i,j = 1, ..., n \qquad (3.5)$$

They are spin independent and obey the commutation rules

$$[\hat{E}_{i,j}, \hat{E}_{k,l}] = \hat{E}_{i,l}\delta_{j,k} - \hat{E}_{k,j}\delta_{i,l}, \quad i,j,k,l = 1, ..., n \qquad (3.6)$$

The diagonal generators $\hat{E}_{i,i}$ are called the weight generators while the off diagonal generators $\hat{E}_{i,j}$ are divided into raising (for $i < j$) and lowering (for $i > j$) generators.

The first two terms in (3.4) are the usual one electron Hückel Hamiltonian:

$$H = \sum_{i,j}^{n} h_{ij} \sum_{\mu}^{2} a^{\dagger}_{i,\mu}\, a_{j,\mu},$$
$$h_{ij} = \begin{cases} \alpha_i & \text{if } i = j \\ \beta_{ij} \neq 0 & \text{between near neighbors only} \end{cases} \qquad (3.7)$$

The other two terms in the full electronic Hamiltonian (3.4) are the Coulomb repulsion between two electrons, of opposite spins, which are on the same site and on adjacent sites, respectively. (The repulsion between different sites decreases with distance between them,[22,30] hence we only include the repulsion between near neighbors).

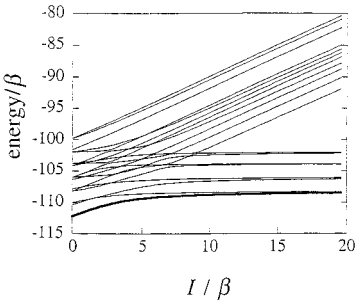

Figure 5. The energy of the twenty adiabatic states of a four-site problem plotted vs the dimensionless ratio x of the Coulomb repulsion energy I to the transfer amplitude β. The energy is shown in units of β and the plot is for the set of site energies (= local ionization potentials) of the radical cation Ala-Ala-Ala-Tyr$^+$, see Table 1 with the same value of I for all the sites. On the left, as $x \rightarrow 0$ is the molecular orbital limit where covalent and ionic states are degenerate. Toward the right, where $x \gg 1$, is the site (or atomic) limit. The energetic role of the Coulomb repulsion is very evident in this regime. Note that the ground state is degenerate in this limit, being made up of states (13) and (17) of (3.1). These are the two states with a positive charge on the chromophore site, which is the site of lowest IP.

Computing the matrix elements of the generators $\hat{E}_{i,j}$ in the site basis is straightforward.[23,27] But the diagonalization of the 20×20 Hamiltonian matrix needs to be done numerically. The results are shown in Figure 5 as a function of the ratio of the Coulomb repulsion I to the charge-transfer coupling β. The parameters of the Hamiltonian that are needed to generate Figure 5 are given in Table 1 in units of β.

We emphasize that the eigenstates we discuss and the results shown in Figure 5 are the many electron states. Figure 5 is not the energies of the molecular orbitals. The Hamiltonian (3.4) explicitly includes electron−electron repulsion terms and so one cannot assign electrons to independent orbitals. We even do not have self-consistent orbitals because we exactly diagonalize the Hamiltonian rather than use a self-consistent procedure. What we generate is a many electron wave function which is expressed as a linear combination of the site many electron states (which are our diabatic basis). From the wave function one can compute expectation values but one cannot think of the electrons independently of one another. This is the price for including Coulomb effects and we cannot ensure a correct dissociation without them.

The essential point in the plot of the adiabatic states in Figure 5 is that while the ground state of the molecular ion is well below the excited states, once there is some excess energy, many excited electronic states are accessible. Textbooks usually show energies in the molecular orbital scheme, where covalent and ionic states are degenerate and thereby one forms the impression that there are fewer states than there really are. In reality, Figure 5 is still an underestimate of the number of states. This is because we allowed only one orbital per site. Each amino acid has excited states and so the number of possible electronic states of the peptidic ion is even higher than shown in Figure 5.

To conclude this section, we have discussed two alternative sets of many electron states. The first is the site (or diabatic) states. These states tell on which site the charge is localized and so are suitable for describing the charge migration. These states do not diagonalize the full electronic Hamiltonian and are coupled by the charge-transfer term, $\beta\sum_{i\neq j=1}^{4}\hat{E}_{i,j}$, of the Hamiltonian. This transfer converts one state into another so the diabatic states are nonstationary. The members of the other set of states that we use are the adiabatic or Born−Oppenheimer states. These diagonalize the electronic Hamiltonian and are stationary electronic states. Each adiabatic state can be expressed as a linear combination of diabatic states and the coefficients of this expansion are determined when we diagonalize the electronic Hamiltonian matrix (which is most readily computed in the diabatic basis, in which it is not diagonal). Conversely, each diabatic state can be expressed as a linear combination of adiabatic states. In other words, the diabatic states are not eigenstates of the electronic Hamiltonian and so are not stationary. As a diabatic state evolves in time one can think of it either in terms of transitions to other diabatic states or, equivalently, as a change in the weights of the adiabatic states. The former description is more useful for the picture where the location of the charge determines the reactivity. The description in terms of changing weights of the adiabatic states is more useful for showing that eventually the electronic motion will decohere.

There are two contributions to the decoherence of the initial state. One is inherently electronic. The unequal energies of the different adiabatic states means that each acquires, in time, a different phase. This effect is taken into account in the present computations. The more do the adiabatic states differ in their energy, the faster is this decoherence. It is for this reason that we emphasize in Figure 5 that excited electronic states are closer in energy than one might have thought. There is an additional contribution to the decoherence due to the nuclear motion and the internal structure of each site. These two effects are not included and are the subject of computations that are in progress.

4. Electronic States of the Dissociation Channels

This section shows that for peptides with a chromophore at the C end, there are four dissociation channels with relatively low threshold, two at the C end and two at the N end. The lowermost threshold for dissociation from the ground state of the cation is at the C end. The reasoning is straightforward. Take (Leu-Leu-Leu-Trp)$^+$ as an example. There are eight site states, shown in (3.1), with a charge missing at the C end. A dissociation channel leading to Leu-Leu-Leu and Trp$^+$ must be made up from these eight basis states. But as discussed following (3.2), of the eight states shown in (3.1), there are only two (degenerate) states of low energy. Next consider dissociation at the N end leading to Leu$^+$ and Leu-Leu-Trp. There are eight site states with a charge missing at the N end. These states are the mirror image of the states shown in (3.1). Again, only two (degenerate) states have a low energy. The two lowest energy channels for dissociation at the N end, leading to Leu$^+$ and Leu-Leu-Trp, have a somewhat higher threshold than the two lowest threshold product channels at the C end. If the local IPs were equal, all these channels would have the same threshold. (Since our sites have no internal structure, our bond energies are equal). But the local IPs are not all the same. Trp has a lower IP than Leu. For the same reason, dissociation channels leading to Leu-Leu-Leu$^+$ and Trp or to Leu and Leu-Leu-Trp$^+$ have a higher threshold than when the charge is on the smaller fragment.

There are other open channels. In particular, note the two states in the bottom row of (3.1). These two states can dissociate to both Leu$^+$ and Leu-Leu-Trp and to Leu-Leu-Leu and Trp$^+$. These two states are ionic. Depending on the value of the Coulomb repulsion I, these states can be at a higher energy.

In summary, of the 20 possible site states of the radical cation, two site states can dissociate at the C end and two different states can dissociate at the N end. The threshold for dissociation at the N end is somewhat higher than at the C end but it too can be reached with three photons of 4.5 eV. Leu-Leu-Leu-Trp$^+$ is observed, Figure 6 and section 7, to dissociate about equally from both ends. All other channels will have higher thresholds and require a four-photon absorption.

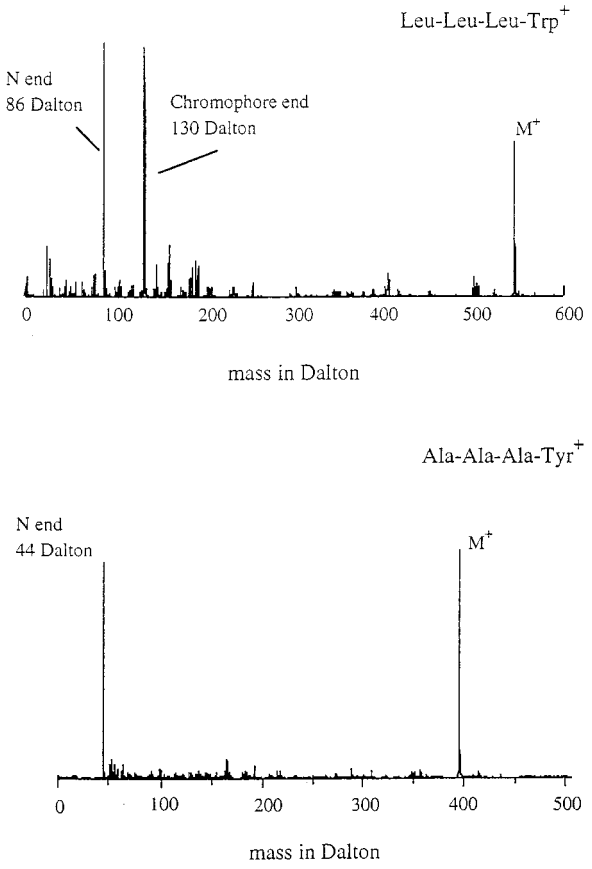

Figure 6. Experimental, see section 7, fragmentation pattern of the tetrapeptides (a) Leu-Leu-Leu-Trp and (b) Ala-Ala-Ala-Tyr following a resonant UV(1+1) ionization and a subsequent UV laser excitation (The laser wavelength for ionization and excitation is 266 nm with a pulse width of 5 ns and intensity of about 10^6 W/cm^2). The fragment ions of mass 86 and 44 dalton are identified as the N terminal immonium cation of Leu and Ala, respectively. The fragment ion of mass 130 is from the C terminal fragmentation of Trp (In the fragment cation, the indole five membered ring presumably isomerizes to a six member one). In (a) dissociation at the N end and at the chromophore (the C end) are both probable. At much higher laser intensities more complex fragmentation is observed and the mass spectral pattern looks more statistical.

The same considerations apply also to our other example, Ala-Ala-Ala-Tyr. On the other hand, the observed, Figure 6, fragmentation patterns of the two peptides are different. Unlike Leu-Leu-Leu-Trp$^+$, Ala-Ala-Ala-Tyr$^+$ dissociates quite preferentially at the N-end.

5. Coupling to the Dissociation Channels

To allow for dissociation and yet to keep the problem discrete one can introduce an effective electronic Hamiltonian which is defined in the same basis of electronic states that describe the bound radical cation. The coupling to the dissociation channels is introduced using a Hermitian rate operator Γ. The effective electronic Hamiltonian H is then given by

$$H = H - i\Gamma \tag{5.1}$$

where H is the electronic Hamiltonian of the bound cation, here given by (3.4). The effective electronic Hamiltonian needs to be diagonalized using a biorthogonal basis and its eigenvalues are complex.[31] In general the rate operator Γ is not diagonal so that the real part of the eigenvalues of H is not equal to the energies of H. In other words, the coupling to the continuum not only endows states with a decay width but also shifts the energies of the states. This section discusses the determination of the matrix elements of the rate operator Γ. The general issue is clear. The rate operator has the generic form

$$\Gamma = \sum_c V_c^\dagger \rho_c V_c \tag{5.2}$$

where V_c is the coupling between the bound states and channel c of the continuum and ρ_c is the density of states in that continuum channel. In particular, when a channel has a higher threshold, it will have a lower density of states.

The identity of electronic channels in the continuum follows from the considerations of section 3. In the basis that we use, of one orbital per site, there are eight channels that correspond to dissociation at the C end, with the charge remaining on the larger fragment. The set of states is that shown in (3.1). The electronic Hamiltonian for these eight product channels is like that of the parent cation, as given in (3.4), except that there is no transfer coupling between sites 1 and 2 nor is there a Coulombic interaction between these sites:

$$H_{\text{frag}}{}^{\text{C}} = \sum_{i=1}^{4} \alpha_i \hat{E}_{i,i} + \beta \sum_{i\neq j=2}^{4} \hat{E}_{i,j} + \frac{1}{2}\sum_{i=1}^{4} \hat{E}_{i,i}(\hat{E}_{i,i} - 1)\, I_i + \frac{\gamma}{2}\sum_{i\neq j=2}^{4} \hat{E}_{i,i}\,\hat{E}_{j,j} \tag{5.3}$$

Similarly, there are eight channels that correspond to dissociation at the N end. The basis is the mirror image of that shown in (3.1). That is, the basis of states that have no charge at the N end. The electronic Hamiltonian for these eight product channels is like that given in (5.3), except that for products at the N terminal there is no transfer coupling between sites 3 and 4 nor is there a Coulombic interaction between these sites.

Note that two channels correspond to dissociation at both the C and the N ends. The two states are shown at the bottom row in (3.1). These two channels can have a higher threshold because they are ionic states (which are penalized by the Coulomb repulsion). At low values of I these states can offer a lower energy route where dissociation is possible at both ends.

As discussed in section 4, of the 14 electronic product channels, four have a low threshold, two each for dissociation at a given end. We retain only these four channels so that the bound-continuum coupling V is a 20×4 matrix. *A la* the Wolfsberg−Helmholz approximation[32] we take this electronic coupling to be proportional to the overlap of the bound and product state electronic wave functions. We have used two different choices for the product wave functions. One choice is what we call the adiabatic choice. The states of the products, say at the C end, are obtained by diagonalizing the product's Hamiltonian, (5.3) above, in the basis of the eight states given in (3.1). For the N end we use an equivalent procedure. The other choice is the diabatic one. The continuum states are the diabatic states of the products. The diabatic choice is appropriate when the dissociation is so very prompt so that there is not enough time for the electronic reorganization of the products during dissociation. Since the experimental results are that dissociation competes with charge migration, one cannot rule out the diabatic choice. The results in section 6 below show that given that the initial ionization was localized then the next most important aspect governing the fragmentation pattern is the specification of the electronic states of the products.

We draw special attention to the possibility raised in the paragraph above, that upon a very fast ionization, the fragmentation pattern can differ as compared to a slower laser pulse

which allows the electrons to reorganize while the pulse is still on. We intend to examine this in detail in view of the experimental results reported in ref 33. The pulse duration in these early experiments is short (500 fs) but not ultrashort. It is clearly of considerable interest to repeat the experiment with even shorter pulses.

6. Computational Results and Discussion

The technical message of the computations is that the specification of the initial state and of the product channels do matter. Not all bound states of the four-site cation will dissociate in the same way nor is it the same to use a diabatic or an adiabatic description of the products. This is over and above the inherent bias that the experiments study the dissociation of peptides with an amino acid of a low ionization potential at the C end. By itself this means that the initial state accessed by the laser can only be one of the eight states with no charge at the C terminal, states shown in (3.1). However, these states evolve under the action of the full Hamiltonian and this evolution takes part during the laser pulse and thereafter. If the laser acts for a longer time, it prepares states with ever-narrower spread in energy. If the ion was stable then a cw laser will prepare a state with a sharp energy. But the states can decay and this requires a more detailed theory.[34,35] Here we forego the complete treatment and instead examine two limiting cases: a nonstationary and a stationary initial states.

The need to specify the details has both advantages and not so good aspects. It is good because it means that one has the option for control over and above the control implied by the ability to synthesize a peptide with a particular sequence of amino acids. Weinkauf et al.[6] have shown that the sequence very much determines the reactivity and the theory is quite consistent with this observation. Here intuition and theory agree in that the role of the sequence is to determine the ease of charge migration. This effect can be accounted for even at the level of a one-electron picture[12] although the role of Coulomb blocking is nonnegligible so that the more realistic Hamiltonian we use here is preferable. The theory further suggests that even for a given sequence, the details of the initial state of the ion do matter and particularly so at higher energies. That the fragmentation pattern at higher energies can be different is not inconsistent with the available experimental results. The computations show that even at lower energies there can be differences. These differences are not extreme because, as discussed in section 4, few product channels are open at low energies. Still, the computational evidence does not allow one to categorically state that a given sequence will, say, preferentially dissociate at the N end irrespective of the precise initial state. This makes the presentation of the computational results more pedantic because one has to specify the particular initial state that is employed and also whether a diabatic or an adiabatic description is adopted for the products.

Computations were carried out by propagating in time, under the full Hamiltonian (5.1) an initial state and computing the fraction of products of dissociation at either the C or the N end. The location of the charge in the undissociated parent ion was also monitored. The results are shown in Figure 7 for Leu-Leu-Leu-Trp$^+$ and in Figure 8 for Ala-Ala-Ala-Tyr$^+$. The most noticeable aspect of the computations is that the nature of the coupling to the continuum, as discussed in section 5, does matter and we therefore specify it in detail.

For both peptides, and using our Hamiltonian to compute energy levels, dissociation at the C end has a somewhat lower threshold. The corresponding density of states is therefore higher. Above any electronic factors we therefore make dissociation at the C end more favorable by a factor of 1/0.64. Other things being equal, dissociation will have a higher yield form the C end. We emphasize this point because the surprising result is that one can have dissociation predominately at the N end, both experimentally and computationally. Specifically we take the partial widths to have the form, cf. (5.2), $\Gamma_X = V_X^\dagger \rho_X V_X$ where $\rho_C = 1/\beta$ and $\rho_N = 0.64/\beta$. The electronic coupling to the continuum is different for the diabatic and adiabatic cases. The two low energy diabatic channels for dissociation are the states 13 and 17, shown as the top row in (3.1), at the C end and states 4 and 6, shown as the top row in (3.3), for the N

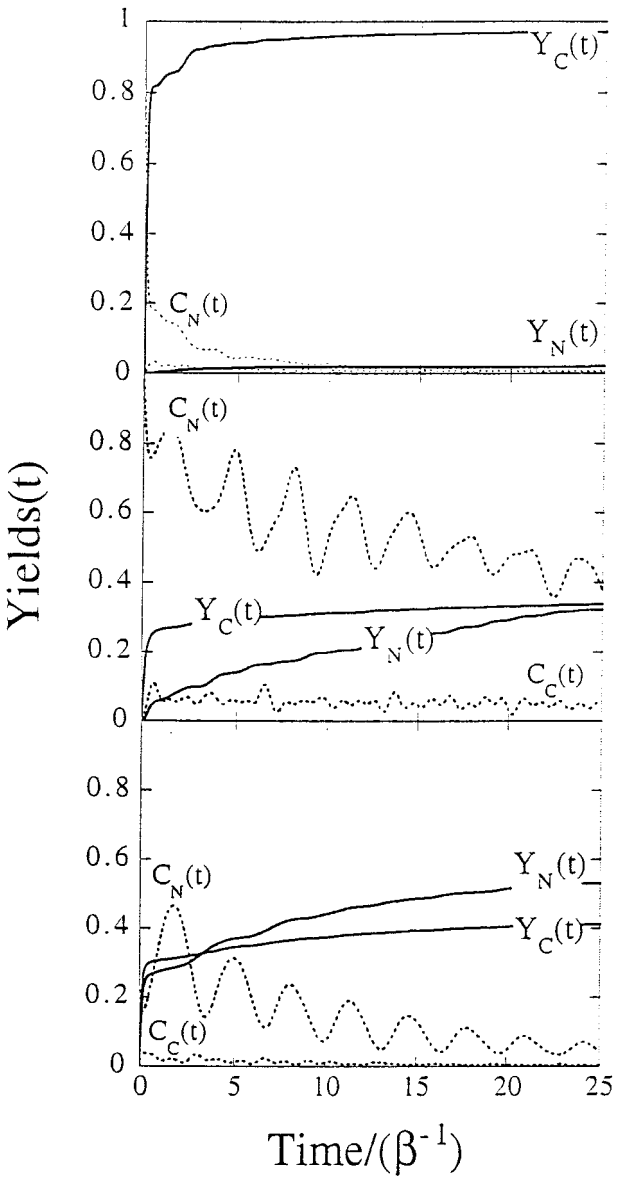

Figure 7. Computed yields of the dissociation at the two ends of Leu-Leu-Leu-Trp$^+$ as a function of time. (We scale energy in units of β so that $1/\beta$ is the reduced unit of time.) Also shown are the negative charges at the two ends (expectation values of $\hat{E}_{i,i}$, $i = 1$ or 4) so as to show that "reactivity follows the (positive) charge". The three panels show the effect of the electronic states of the continuum and of the initial state, with more details provided in the text. (a) Diabatic product states and a diabatic initial state as is expected to be the case for a fast ionization. (b) Adiabatic products states and the same initial state as in (a). Note the remarkable change in the selectivity. (c) Adiabatic product states and an adiabatic initial state which is the state correlated with the diabatic state used in (a) and (b). Note that the selectivity is not too different from that in (b).

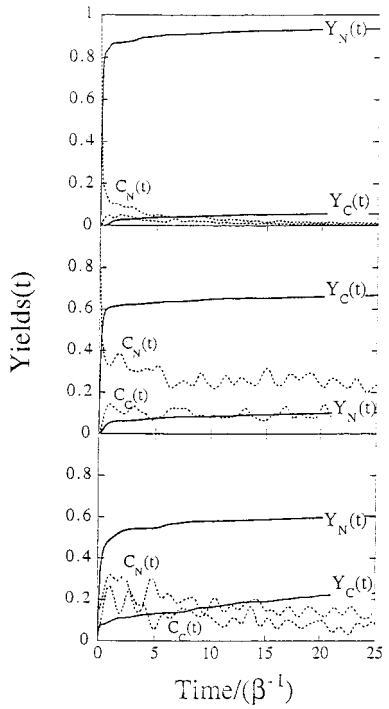

Figure 8. Computed yields of the dissociation at the two ends of Ala-Ala-Ala-Tyr $^+$ as a function of time. (We scale energy in units of β so that $1/\beta$ is the reduced unit of time.) Also shown are the negative charges at the two ends, as in Figure 7. The three parts show the effect of the electronic states of the continuum and of the initial state, with more details provided in the text. (a) Diabatic product states and a diabatic initial state as is expected to be the case for a fast ionization. (b) Adiabatic products states and the same initial state as in (a). (c) Adiabatic product states and an adiabatic initial state which is the state correlated with the diabatic state used in (a) and (b). Note the dramatic change in selectivity: the dissociation occurs now preferentially from the N end.

end. The low energy adiabatic channels are obtained by diagonalizing the fragments Hamiltonian, e.g., (5.3) for dissociation at the C end, and taking the lowest channels for each end.

For Leu-Leu-Leu-Trp$^+$ dissociation is very much favored at the C end when diabatic product channels are used. When adiabatic product channels are used, dissociation occurs roughly equally from both ends. As discussed below, we attribute this difference to the role of the ionic states which reflects the ability of Leu, as compared to Ala, to better accommodate two electrons. For Ala-Ala-Ala-Tyr $^+$, too, dissociation is very much favored at the C end when diabatic product channels are used. But when adiabatic product channels and an adiabatic initial state are used, dissociation occurs preferentially from the N end. This is because of the higher charging energy of Ala so that charge does not accumulate in the middle and is rapidly transferred to the other end.

In Figures 7 and 8 we show computational results corresponding to propagating an initial state in time, using the full Hamiltonian which includes the electronic Hamiltonian and the coupling to the dissociation channels. Here we provide a qualitative discussion.

Consider first the very prompt dissociation. An initial state accessed in the experiment of Weinkauf and Schlag has the charge localized at the chromophore end. Such an initial state is either one of the eight states shown in (3.1) or a linear combination of these states. In quantitative terms the initial state is a vector $\mathbf{c}$ of twenty components. Each component of $\mathbf{c}$ specifies the amplitude (weight = |amplitude|^2) of the Weinkauf and Schlag initial state on one of the twenty different states of the radical cation in the site basis. Twelve components of $\mathbf{c}$ are identically zero because the initial state produced in the experiment of Weinkauf and Schlag has the charge localized at the chromophore end and only eight basis states answer to that description.

Let $\mathbf{d}_C$ be a low energy state that dissociates promptly at the C terminal where the subscript is a reminder of which end it dissociates from. $\mathbf{d}_C$ is a vector of 20 components, but since $\mathbf{d}_C$ is one of the low threshold states, then only two of its components will be nonzero. Will the initial state $\mathbf{c}$, the initial state of relevance to the experiment, dissociate promptly at the chromophore end? Yes, if it has a high overlap with $\mathbf{d}_C$ and no, otherwise. So the measure of prompt dissociation at the chromophore end is $\mathbf{c}^T \cdot \mathbf{d}_C$. Let $\mathbf{d}_N$ be a low energy state that dissociates promptly at the N terminal. Then the magnitude of the overlap $\mathbf{c}^T \cdot \mathbf{d}_N$ determines if the experiment shows prompt dissociation at the N terminal. This scalar product vanishes if $\mathbf{c}$ is one of the eight states with no electron at the C terminal, because if $\mathbf{d}_N$ has no electron on the N terminal, it is a low energy state having an electron at the C terminal.

The prompt fragmentation pattern of an initial state $\mathbf{c}$ is determined by its overlap with the site basis states. There are four site states that dissociate with a low threshold. Two dissociate preferentially at the C end and two at the N end. An initial state with no charge at the C end will not overlap with the low threshold states that dissociate promptly at the N end. A low energy initial state with no charge at the C end will preferentially dissociate at the N end only if charge migration does take place prior to dissociation.

We emphasize that it can be that an initial state with no charge at the C end can promptly dissociate at the N end. This is possible at such energies where one can access the ionic states (bottom row in (3.1)) where the electrons are localized in the middle so that negative charge is absent at both ends. The point of the experiment is that dissociation at the N end is observed even at low levels of excitation and so the fragmentation pattern can be used as a signature of charge migration.

At lower energies, dissociation at the N end is possible only if during or after the laser pulse the initial state with a charge missing at the C end evolves under the full Hamiltonian. That reactivity follows the charge is evident from Figures 7 and 8. Very prompt dissociation occurs only while the positive charge remains localized on its initial site. Thereafter one sees dissociation at that end where the charge is, as can be seen in particular from the almost steplike increase in the yield when the positive charge arrives. At longer times, the initial state decoheres and the steplike behavior is smoothed out.

After the charge has had the time to swing to the other end and back a few times, it becomes about equally distributed over both ends and dissociation can occur from both. It is however often the case that by that time many or even most of the parent molecules have already dissociated. This is because the strength of coupling to the continuum that we use is of the order of magnitude of the charge-transfer integral β. (Γ is of the order of $V^2\rho$). Dissociation can therefore compete with charge transfer. It is because of this competition that details do matter. If charge transfer was very much faster one will see dissociation from both ends, while if the charge remained largely localized, dissociation will occur very preferentially at the C end. At higher energies of excitation, where ionic states can very effectively move charge from one end to the other, a statistical behavior is expected.

7. Experimental Aspects

For a test of the model, nanosecond laser pulse fragmentation spectra have been recorded. The experimental setup is described in detail elsewhere.[5,6] In short, neutral peptides were laser-desorbed in a channel (1 mm diameter) and by a pulse of Ar carrier gas transported into the ion source of a reflectron time-of-flight mass spectrometer. A pulsed nozzle forms the pulse of Ar carrier gas. The nozzle backing pressure is typically 3 bar. During the transport and the expansion into vacuum collisions between probe molecules and carrier gas provide efficient cooling of internal degrees of freedom. The ion source is set to a high extraction voltage to allow admittance of neutral molecules only. Ionization is performed by resonant UV(1+1) ionization via the chromophore S_1 states of tyrosine (Tyr) and tryptophan (Trp). The laser pulse width is 5 ns. Ionization is local at the chromophore and usually fragment-free ionization can be performed at low laser intensities (about 10^5 to 3×10^5 W/cm^2. Cation excitation is then performed by a simple increase of the laser intensity to about to 10^6 W/cm^2. From intensity variations we have evidences that the cation absorbs one UV photon (photon energy about 4.5 eV).

Figure 6 showed the observed fragmentation pattern for (a) Leu-Leu-Leu-Trp and (b) Ala-Ala-Ala-Tyr. Both peptides have a chromophoric amino acid at the C end (Trp or Tyr) and nonaromatic amino acids (leucine, Leu; alanine, Ala) at the N terminal. As was discussed in the Introduction and further on, these examples in themselves show that charge does migrate. Also, the observed differences in the fragmentation patterns for the two cases can be interpreted in zeroth order by a local picture which predicts equal threshold energies for dissociation at both terminals for the Leu-Leu-Leu-Trp cation but a lower dissociation threshold at the N terminal of the For Ala-Ala-Ala-Tyr cation.

The nanosecond laser excitation and the mass-spectrometric detection are not able to resolve any possible time structure in dissociation as possibly caused by fast charge migration (or electronic state population). Hence, the present experimental results only provide the time-accumulated fragment ion intensities. These can be used for comparison with the calculated long time yields. In future work we intend to measure fragmentation patterns of model small peptides determined using short pulse lasers. Such experiments will allow an examination of the above-discussed computed differences between ultrashort and longer ionization pulses.

8. Summarizing Remarks

The concept of charge directed reactivity has been examined for a simple electronic model and using a basis of states where the location of the charge is well defined. The peptide has been mimicked as a chain of sites, with a chromophore at the C terminal, where the chromophore is the site with the lowest local ionization energy. The electronic Hamiltonian includes both on-site and inter-site Coulombic effects and a charge-transfer term that moves the charge between adjacent sites. Including the Coulomb repulsion resolves the degeneracy of the covalent and ionic states which is characteristic of simple molecular orbital theory and allows for a proper description of the dissociation channels. The competition between charge migration and dissociation has been demonstrated by computational results and has been discussed. In particular it is argued that this competition allows for a bypass of the RRKM scenario. The diabatic electronic states do not make the energy available for a rapid intramolecular transfer among the vibrational modes. Comparison has been made with the experimental results for the dissociation of the tetra peptide cations Leu-Leu-Leu-Trp$^+$ and Ala-Ala-Ala-Tyr$^+$.

Acknowledgment. We thank H. Kessler and co-workers for sample synthesis. This work was supported by SFB 377 and by the Volkswagen Foundation. F.R. thanks the Fonds de la Recherche Fondamentale Collective, Belgium.

References and Notes

(1) Oref, I.; Rabinovitch, B. S. *Acc. Chem. Res.* **1979**, *12*, 166.
(2) Wilson, K. R.; Levine, R. D. *Chem. Phys, Lett.* **1988**, *152*, 435.
(3) Lifshitz, C. *Int. Rev. Phys. Chem.* **1997**, *16*, 113.
(4) Schlag, E. W.; Levine, R. D. *Chem. Phys. Lett.* **1989**, *163*, 523.
(5) Weinkauf, R.; Schanen, P.; Yang, D.; Soukara, S.; Schlag, E. W. *J. Phys. Chem.* **1995**, *99*, 11255.
(6) Weinkauf, R.; Schanen, P.; Metsala, A.; Schlag, E. W.; Buergle, M.; Kessler, H. *J. Phys. Chem.* **1996**, *100*, 18567−18585.
(7) Weinkauf, R.; Schlag, E. W.; Martinez, T. J.; Levine, R. D. *J. Phys. Chem. A* **1997**, *101*, 7702−7710.
(8) Remacle, F.; Levine, R. D. *J. Phys. Chem. A* **1998**, *102*, 10195−10198.
(9) Diau, E. W.-G.; Herek, J. L.; Kim, Z. H.; Zewail, A. H. *Science* **1998**, *279*, 847−851.
(10) Hose, G.; Taylor, H. S. *Chem. Phys.* **1983**, *84*, 375−392.
(11) Remacle, F.; Lorquet, J. C.; Levine, R. D. *Chem. Phys. Lett.* **1993**, *209*, 315−324.
(12) Remacle, F.; Ratner, M. A.; Levine, R. D. *Chem. Phys. Lett.* **1998**, *285*, 25−33.
(13) Miller, W. H. *J. Chem. Phys.* **1976**, *65*, 2216.
(14) Pollack, E.; Levine, R. D. *J. Phys. Chem.* **1982**, *86*, 4931.
(15) Levine, R. D.; Bernstein, R. B. *Molecular Reaction Dynamics and Chemical Reactivity*; Oxford University Press: Oxford, 1987.
(16) Rosenstock, H. M.; Wallenstein, M. B.; Warhaftig, A. L.; Eyring, H. *Proc. Natl. Acad. Sci.* **1952**, *38*, 667.
(17) Lorquet, J. C. *Mass Spectrom. Rev.* **1994**, *13*, 233−257.
(18) Illenberger, E.; Momigny, J. *Gaseous Molecular Ions*; Springer-Verlag: New York, 1992; Vol. 2.
(19) Holbrook, K. A.; Pilling, M. J.; Robertson, S. *Unimolecular Reactions*, 2nd ed.; John Wiley & Sons: Chichester, 1996.
(20) Hubbard, J. *Proc. R. Soc.* **1963**, *276*, 238−257.
(21) Matsen, F. A. *Int. J. Quantum Chem.* **1990**, *37*, 389−402.
(22) Parr, R. G. *Quantum Theory of Molecular Electronic Structure*; Benjamin: New York, 1963.
(23) Paldus, J. *J. Chem. Phys.* **1974**, *61*, 5321−5330.
(24) Matsen, F. A. *J. Chem. Educ.* **1985**, *62*, 367−373.
(25) Coulson, C. A.; Fischer, I. *Philos. Mag.* **1949**, *40*, 386.
(26) Pariser, R. *J. Chem. Phys.* **1956**, *24*, 250−256.
(27) Remacle, F.; Levine, R. D. *J. Chem. Phys.* **1999**, 5089−5099.
(28) Newton, M. D.; Sutin, N. *Annu. Rev. Phys. Chem.* **1984**, *35*, 437.
(29) Lindenberg, J.; Öhrn, Y. *Propagators in Quantum Chemistry*; Academic Press: New York, 1973.
(30) Paldus, J.; Li, X. *Isr. J. Chem.* **1991**, *31*, 351−362.
(31) Levine, R. D. *Quantum Mechanics of Molecular Rate Processes*; Oxford University Press: Oxford, 1969.
(32) Wolsberg, M.; Helmholz, L. *J. Chem. Phys.* **1952**, *20*, 837.
(33) Weinkauf, R.; Aicher, P.; Wesley, G.; Grotemeyer, G.; Schlag, E. W. *J. Phys. Chem.* **1994**, *98*, 8381.
(34) Remacle, F.; Levine, R. D. *J. Chem. Phys.* **1997**, *107*, 3382−3391.
(35) Shapiro, M. *J. Phys. Chem.* **1998**, *102*, 9570−9576.